

Incidence of Electric Field and Sulfuric Acid Concentration in Electrokinetic Remediation of Cobalt, Copper, and Nickel in Fresh Copper Mine Tailings

Authors:

Rodrigo Ortiz-Soto, Daniela Leal, Claudia Gutierrez, Alvaro Aracena, Marcelo León, Andrea Lazo, Pamela Lazo, Lisbeth Ottosen, Henrik Hansen

Date Submitted: 2023-02-17

Keywords: electrokinetic remediation, heavy metal removal, mine tailing

Abstract:

In the present study, the assessment of heavy metal contaminant migration from fresh mine tailings was conducted using the electrokinetic remediation technique (EKR). In this sense, a pilot EKR cell was designed to evaluate the recovery potential of copper, nickel, and cobalt species. In particular, the focus was on the impacts of electric field intensity and pH in initial mixture and testing their interaction in copper, nickel, and cobalt migration. Experiments were made using a 22 factorial experimental design with a central point, using DC electric fields from 1.0 to 2.0 V cm⁻¹ and H₂SO₄ pretreatment solutions from 1.0 to 2.0 mol L⁻¹, along with an ANOVA test with error reduction. The metal removal rates were approximately 7% for cobalt, neglectable for copper, and 6% for nickel. In the best cases, the highest concentrations by migration at the cathodic zone were 11%, 31%, and 30%, respectively. According to ANOVA tests, factor interaction was proven for each metal in the half cell near the cathode and the closest zone from the cathode specifically. Both factors affected metal concentrations, which indicates that when the goal aims for species accumulation in a narrower section, each factor has a significant effect, and their interaction makes a proven enhancement. Thus, using 2.0 V cm⁻¹ and 2.0 mol L⁻¹ showed a high improvement in metal concentration in the cathodic zone.

Record Type: Published Article

Submitted To: LAPSE (Living Archive for Process Systems Engineering)

Citation (overall record, always the latest version):

LAPSE:2023.0166

Citation (this specific file, latest version):

LAPSE:2023.0166-1

Citation (this specific file, this version):





LAPSE:2023.0166-1v1

DOI of Published Version: <https://doi.org/10.3390/pr11010108>

License: Creative Commons Attribution 4.0 International (CC BY 4.0)

Article

Incidence of Electric Field and Sulfuric Acid Concentration in Electrokinetic Remediation of Cobalt, Copper, and Nickel in Fresh Copper Mine Tailings

Rodrigo Ortiz-Soto ^{1,*}, Daniela Leal ², Claudia Gutierrez ², Alvaro Aracena ¹, Marcelo León ¹, Andrea Lazo ², Pamela Lazo ³, Lisbeth Ottosen ⁴ and Henrik Hansen ²

¹ Escuela de Ingeniería Química, Pontificia Universidad Católica de Valparaíso, Avenida Brasil 2162, Valparaíso 2340025, Chile

² Departamento de Ingeniería Química y Ambiental, Universidad Técnica Federico Santa María, Avenida España 1680, Valparaíso 2390123, Chile

³ Instituto de Química y Bioquímica, Facultad de Ciencias, Universidad de Valparaíso, Avenida Gran Bretaña 1111, Valparaíso 2360102, Chile

⁴ Department of Civil Engineering, Technical University of Denmark, 2800 Kongens Lyngby, Denmark

* Correspondence: rodrigo.ortiz@pucv.cl; Tel.: +56-32-2372645

Abstract: In the present study, the assessment of heavy metal contaminant migration from fresh mine tailings was conducted using the electrokinetic remediation technique (EKR). In this sense, a pilot EKR cell was designed to evaluate the recovery potential of copper, nickel, and cobalt species. In particular, the focus was on the impacts of electric field intensity and pH in initial mixture and testing their interaction in copper, nickel, and cobalt migration. Experiments were made using a 2² factorial experimental design with a central point, using DC electric fields from 1.0 to 2.0 V cm⁻¹ and H₂SO₄ pretreatment solutions from 1.0 to 2.0 mol L⁻¹, along with an ANOVA test with error reduction. The metal removal rates were approximately 7% for cobalt, neglectable for copper, and 6% for nickel. In the best cases, the highest concentrations by migration at the cathodic zone were 11%, 31%, and 30%, respectively. According to ANOVA tests, factor interaction was proven for each metal in the half cell near the cathode and the closest zone from the cathode specifically. Both factors affected metal concentrations, which indicates that when the goal aims for species accumulation in a narrower section, each factor has a significant effect, and their interaction makes a proven enhancement. Thus, using 2.0 V cm⁻¹ and 2.0 mol L⁻¹ showed a high improvement in metal concentration in the cathodic zone.

Keywords: electrokinetic remediation; heavy metal removal; mine tailing



Citation: Ortiz-Soto, R.; Leal, D.; Gutierrez, C.; Aracena, A.; León, M.; Lazo, A.; Lazo, P.; Ottosen, L.; Hansen, H. Incidence of Electric Field and Sulfuric Acid Concentration in Electrokinetic Remediation of Cobalt, Copper, and Nickel in Fresh Copper Mine Tailings. *Processes* **2023**, *11*, 108. <https://doi.org/10.3390/pr11010108>

Academic Editor: Xiaoqiang Cui

Received: 11 December 2022

Revised: 25 December 2022

Accepted: 27 December 2022

Published: 30 December 2022



Copyright: © 2022 by the authors. Licensee MDPI, Basel, Switzerland. This article is an open access article distributed under the terms and conditions of the Creative Commons Attribution (CC BY) license (<https://creativecommons.org/licenses/by/4.0/>).

1. Introduction

Heavy metals in soils are a complex, worldwide, urgent issue due to their toxicity and persistence [1]. Regarding mine tailings, given their magnitude and variety of heavy metals, their natural mechanisms of diffusion/advection allow them to be transported away from their confinement [2,3], risking various elements of ecosystems, such as water reservoirs [4], food [5], and the first link in the marine trophic chain [6], which directly impacts human health and the environment.

The mining industry has contributed immensely to the generation of heavy-metal-containing residues, including cobalt and nickel, which both have moderate toxic effects [7–9]. Therefore, every effort to remove these residues from the environment—including preventing their emanation, if possible—is urgent, especially when mining waste disposal methods are being revised to make mining a more sustainable industry [10,11]. To achieve removal of the residues, several technologies have been developed aiming for control and/or remediation, such as soil flushing, biological processes such as phytoremediation [12] and

bioremediation [13], and electrochemically assisted processes, especially electrokinetic remediation (EKR) [14–16]. Although each technology has its benefits, soil flushing has problems due to the extent of extraction agents, and phytoremediation/bioremediation has complications in mine tailings because of a lack of nutrients. When phytoremediation and bioremediation are effective, they carry a potential risk of reintroducing these pollutants in the local trophic chain. On the other hand, the application of electricity allows the migration of ions contained in the liquid phase or available on the solid surface, regardless of how low their concentrations are. Therefore, this technology can transform mining residues into a potentially profitable asset regardless of energy consumption, since it can extract valuable inorganic species from depleted sources and can be applied in situ without the need to modify tailing dams. These advantages, in a global remediation market worth USD 30 billion [17], can make it more economically attractive. A few studies have been performed in mine tailings with this technology [18–24], also specifically in Chilean mine tailings [25–30], typically using a strong acid such as sulfuric acid to extract metals from the solid phase. The most fundamental factors in EKR are the electric field and acid concentration in the pretreatment solutions, even though this analysis has been conducted in one prior study [31], but it checked only one of the EKR sections.

For the aforementioned reasons, this study aims to establish the effect of the pH of the initial mixture (mine tailings with a 20% humidity by using an acid solution) and the electric field intensity applied between the electrodes in the metal migration yield in an EKR cell by identifying and assessing their interaction. A 2²-factorial experimental design has been applied with a central point, in which the factors are the intensity of the electric field and the sulfuric acid concentration in the pretreatment solution, and an ANOVA test was performed in every partition of the cell, in addition to a MonteCarlo simulation for error reduction and migration difference verification between partitions and between experiments.

This statistical approach, which aims to establish more reliable conclusions with a better error propagation control, has never been applied in this way to fresh Chilean copper mine tailings for copper migration. Furthermore, cobalt and nickel EKR in this kind of solid have never registered before.

2. Materials and Methods

2.1. Tailing Samples and Reagents

Mine tailing samples were obtained from a copper processing plant in northern Chile, in the Punta del Cobre belt. According to del Real [32], copper ores from this region normally present copper as Chalcopyrite CuFeS₂, and the cobalt and nickel content normally appears in pyritic matrix by substitution Fe(Co,Ni)S₂. The sample was dried at 105 °C for several days until a constant weight was achieved, and the sample was pulverized in a ball mill to reduce particle size to below 500 microns, thus making it all a uniform size. Solid main characteristics are detailed in Table 1.

Table 1. Sample metal content, pH, and particle diameter.

Parameter	Value
pH	8.04 ± 0.06
Particle diameter, µm	212–350
Cu total concentration, mg kg ⁻¹	486.50 ± 5.50
Co total concentration, mg kg ⁻¹	89.10 ± 5.50
Ni total concentration, mg kg ⁻¹	31.00 ± 1.40

H₂SO₄ (95%, analytic grade) was used to make different solutions used in this study: 5% (v/v) and 1.0, 1.5, and 2.0 mol L⁻¹ each. Additionally, HNO₃ (65%, analytic grade) was used to form a 1:1 solution in volume, equivalent to 7.17 mol L⁻¹. CaCl₂ was used to form a 0.01 mol L⁻¹ solution. HCl (37%, analytic grade) was needed without previous dilution. Distilled water was used when needed for every solution described.

2.2. Experimental Disposal and Measuring

As in Figure 1, an acrylic cell was used as a three-chamber container, separated by n° 131 filter paper. In the central chamber, a wet tailing (20% mass of H₂SO₄ solution to achieve solid saturation) sample was placed. In each extreme chamber, titanium electrodes and electrolytes were added from H₂SO₄ solutions, setting pH at 2 for the cathodic chamber and 4 for the anodic chamber. Each electrode was connected to an Extech 382,285 power supply and an Aktatum AMM-1139 multimeter. During operation, electrolytes were monitored and controlled during day hours via measurement of pH. To avoid hydroxide precipitation in the cathode, a few drops of sulfuric acid solution were added when needed. No pH control was possible during the night.

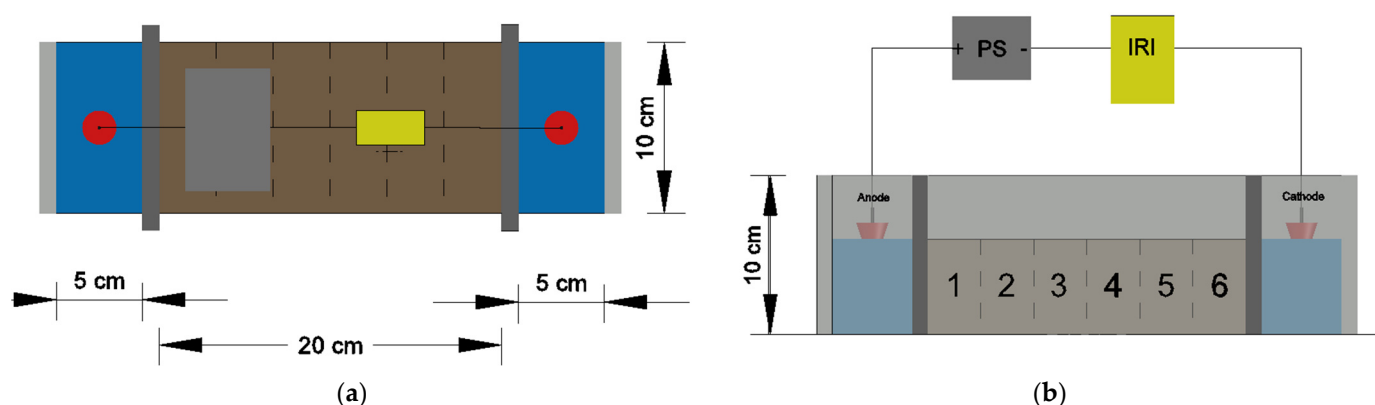


Figure 1. EKR cell disposal. PS: power source. IRI: multimeter with data acquisition. (a) upper view; (b) front view. Numbers 1 through 6 are partitions used for measuring concentration results.

In each seven-day experiment, different sulfuric acid concentrations—the initial sample pH values of which varied from below 4.0 to 7.0, which allowed a different metal solubilization and electric field strength—were used. It was expected that a different metal migration extent for copper would result from varying the applied current; therefore, their current densities in five combinations are shown in Table 2. Effective operation time represents the time during which electrical current is applied through the cell before complete passivation. However, even with different effective times in some experiments, the electrical currents are in a similar range, and some experiments are comparable in these parameters. When the operation was completed, humid soil samples were taken from central chamber; divided into each one of six equal length partitions, as shown in Figure 1; numbered from 1 (nearest to anode) to 6 (nearest to cathode); and dried at 105 °C for 24 h. Next, total and soluble metal contents were measured in duplicate.

Table 2. Experimental design.

Experimental Number	Electric Field V cm ⁻¹	H ₂ SO ₄ Concentration mol L ⁻¹	Sample pH at Beginning of Trial	Average Electrical Current mA	Effective Operation Time Days
1	1.0	1.0	6.93 ± 0.04	45.21	7.0
2	1.0	2.0	3.91 ± 0.02	157.48	7.0
3	2.0	1.0	7.04 ± 0.01	85.57	6.1
4	2.0	2.0	3.79 ± 0.03	339.63	7.0
5	1.5	1.5	4.51 ± 0.03	107.12	4.7

Total and soluble metal concentrations were determined for each partition and for the initial sample of mine tailing. In the case of total content, Danish Standard DS259:2003 was used by taking a 1 g sample of dried solid with 1:1 volume HNO₃ solution and placing the capped flask into the autoclave for 1 h at 200 kPa and 120 °C. Once the flask was cold, the solution was vacuum filtered with 0.45 µm filter paper, and distilled water was added to the filtered solution to make up 100 mL.

For the soluble content, 5 g of each sample was mixed with a 5% (v/v) H₂SO₄ solution for 30 min then vacuum filtered with 0.45 µm filter paper. Then, the filtered solution was mixed with 10 mL of HCl to form a 100 mL solution by adding distilled water. Liquid solutions in both cases were taken for measurement in Flame absorption spectrophotometry (AAS) in a Thermo Scientific M5 spectrometer.

2.3. Calculations

In EKR, a series of process performance indicators are usually required and are related to relevant species migration assessment throughout the entire cell, besides the need for statistical veracity conclusions. In this paper, the process is described in the following text.

2.3.1. Process Indicators

In this study, two indicators of metal ion movement were used, namely normalized metal concentration (κ) (Equation (1)) and global removal (Equation (2)).

$$\kappa_{e,I} = C_{e,i} / C_{e,initial} \quad (1)$$

$$\text{Total removal}_e = (m_{e,initial} - m_{e,final}) / m_{e,initial} \cdot 100\% \quad (2)$$

where C is the concentration (in mg kg⁻¹) and m is the mass (in mg) throughout the whole cell. The subscript e indicates the species (Co, Cu, or Ni), and the subscript i indicates the partition considered (1 to 6), which are the solid sections of the cell central chamber in which each measurement was made after every EKR experiment, aiming for a description of their trajectory, as described in Figure 1.

2.3.2. Statistical Indicators

To ensure more solid conclusions, the statistical design of the experiments was utilized to determine the analyzed factors' effects: an Analysis of Variance [33] (ANOVA) was performed with 10% significance in every normal metal concentration (each metal and each partition, total and soluble), calculated as *p*-values (Equation (3)).

$$p - \text{Value} = P(F > f_{0,u,v}) = \int_{f_{0,u,v}}^{\infty} f(x) dx \quad (3)$$

where *f*(*x*) is Fisher's probability distribution with *u* degrees of freedom in the numerator and *v* degrees of freedom in the denominator. *f*_{0,*u,v*} is the variance ratio between each analyzed factor and experimental error. When the *p*-value is lower than the significance level, the incidence of the factor in metal concentration in a particular partition is proven, with each factor as follows: electric field, acid concentration in pretreatment solution, and their interactions.

In order to establish significant differences in statistical terms, confidence intervals are needed. Since the sample data are reduced, statistically accurate conclusions are limited. Nonetheless, it is possible to mitigate its effect using the Monte Carlo method [34].

The sample standard deviation was calculated according to Equation (4) for each direct measurement.

$$s_{C_{m,i}} = \sqrt{\frac{(C_{m,i_1} - \bar{C}_{m,i})^2 + (C_{m,i_2} - \bar{C}_{m,i})^2}{n - 1}} \quad (4)$$

where *s*_{*C*_{*m,i*}} is the sample standard deviation for each metal *m* of normalized concentration in partition *i* (or initial), *C*_{*m,i*₁} and *C*_{*m,i*₂} are the measurements of each replicate, and $\bar{C}_{m,i}$ is the average concentration of both replicates, all in mg kg⁻¹; *n* is the sample size.

Then, 3000 sets of 100 numbers were generated with the generator from Microsoft Excel[®] using a normal distribution, where the population means and the standard deviations were their corresponding average concentrations and sample standard deviation in each case, respectively.

Later, each standard deviation of the normalized concentrations was determined from their indirect standard error, considering independence between samples (Equation (5)).

$$\alpha_{\kappa_{m,i,s,r}} = \sqrt{\left(\alpha_{C_{m,i,s,r}}/\bar{C}_{m,0,s,r}\right)^2 + \left(-\alpha_{C_{m,0,s,r}} \cdot \bar{C}_{m,i,s,r}/\bar{C}_{m,0,s,r}^2\right)^2} \quad (5)$$

where $\alpha_{\kappa_{m,i,s,r}}$ is the standard error for each metal m of normalized concentration in partition i , from experiment s . For the set r , $\alpha_{C_{m,i,s,r}}$ and $\alpha_{C_{m,0,s,r}}$ are the standard error of each metal of m concentration in partition i (or initial) for the experiment, respectively, from experiment s . Each one was calculated by dividing the sample standard deviation by the square root of 100. $\bar{C}_{m,i,s,r}$ and $\bar{C}_{m,0,s,r}$ are the average concentrations of each partition and initial in mg kg^{-1} .

Finally, the confidence interval, with a confidence level of 90%, is shown for each normalized concentration and difference between each possible pair (Equations (6) and (7)), respectively.

$$\kappa'_{m,i,s} = \frac{\sum_{r=1}^{3000} \left(\frac{\bar{C}_{m,i,s,r}}{\bar{C}_{m,0,s,r}} \pm t_{5\%,99} \cdot \alpha_{\kappa_{m,i,s,r}}\right)}{3000} = \bar{\kappa}_{m,i,s} \pm 1.660 \cdot \bar{\alpha}_{\kappa_{m,i,s}} \quad (6)$$

$$\kappa'_{m,i,s} - \kappa'_{m,j,b} = \bar{\kappa}_{m,i,s} - \bar{\kappa}_{m,j,b} \pm t_{5\%,DF} \cdot \sqrt{\bar{\alpha}_{\kappa_{m,i,s}}^2 + \bar{\alpha}_{\kappa_{m,j,b}}^2} \quad (7)$$

where $\kappa'_{m,i}$ and $\kappa'_{m,j}$ are the population means of normalized concentrations of metal m in partitions i and j for the experiments s and b , respectively. $\bar{\kappa}_{m,i,s}$ and $\bar{\kappa}_{m,j,b}$ are the average of the 3000 sets of normalized metal m in partitions i or j for experiments s and b , respectively. $\bar{\alpha}_{\kappa_{m,i,s}}$ and $\bar{\alpha}_{\kappa_{m,j,b}}$ are the average indirect standard errors. $t_{5\%,99}$ is the t-Student statistic parameter for bilateral confidence intervals for the chosen confidence level and 99 degrees of freedom. $t_{5\%,DF}$ is the same parameter type, but it is calculated for the confidence interval for differences between population means [33], considering equal variances between both treatments (Equation (8)).

$$DF = \left[\frac{\left(\bar{\alpha}_{\kappa_{m,i}}^2 + \bar{\alpha}_{\kappa_{m,j}}^2\right)^2}{\bar{\alpha}_{\kappa_{m,i}}^4 + \bar{\alpha}_{\kappa_{m,j}}^4} \cdot 99 \right] \quad (8)$$

For concentration profiles, error bars are calculated from confidence intervals as Equation (6), and total removals are exhibited with their respective confidence intervals by the same method.

3. Results and Discussion

3.1. Cobalt

Indicators of cobalt total concentration achieved by experiments are shown in Figure 2. It was not possible to detect soluble concentrations of cobalt throughout the EKR cell, except for partition 6 in experiment 4, in which a concentration of $4.16 \pm 0.30 \text{ mg kg}^{-1}$ was observed. This phenomenon can be suggested from the work of del Real et al. [32] since the principal copper ore from the Punta del Cobre belt, where the sample is from, is Iron Oxide Copper-Gold (IOCG). In this kind of copper ore, cobalt is commonly present as sulfide, and in this mineral, the cobalt solubilization is extremely low, even in acidic environments [35].

After analyzing the results, cobalt migration was not observed in experiments 1, 2, and 5 since there are no statistically significant differences between any couple partitions. This was observed by noticing that all error bars for those experiments shared common values. Regarding experiment 3, partition 1 is significantly lower than any other partition near the cathode in the same experiment considering the error bars of partition 1 are lower than for partitions 4, 5, and 6. Between any other pair, this difference is not proven; thus, cobalt depletion was proven near the anode and migrated to every other partition equally. These results suggest that cobalt removal, at least from the anodic zone, is more influenced by

voltage drop than acid concentration. In the case of experiment 4, partition 6 is significantly higher than any other partition in that experiment because its error bars are considerably higher than other partitions. Therefore, in this experiment, cobalt migration was observed seemingly from every cell sector to partition 6.

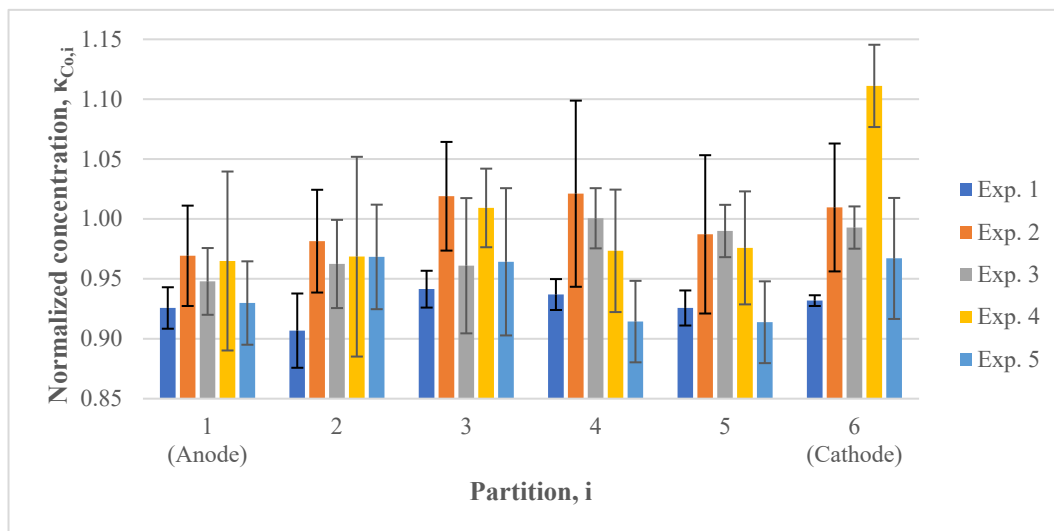


Figure 2. Total cobalt concentration profiles.

When comparing experiments, there is no difference in partition 1 for any experiment; therefore, cobalt removal in the anodic zone is indifferent to analyzed operating conditions. Regarding partition 6, results showed that experiment 4 raises cobalt concentration higher than any other experiment, and experiment 1 presents lower concentrations than experiments 2 and 3. This indicates that the most aggressive operation conditions are more effective in concentrating this species in the cathodic zone, reaching an 11% augmentation. On the other hand, minimally aggressive conditions are less effective in cobalt accumulation near the cathode than when a higher electric field or more acid initial solution is used. In addition, no difference was observed in this partition between experiments 2, 3, and 5. It can be suggested that their conditions are equivalent in the aim of concentrating cobalt near the cathode. From these results, it can be observed that cobalt migration is strongly promoted by using an electric field of 2.0 V cm^{-1} and a 2.0 mol L^{-1} acid solution, and this migration is not affected by anode proximity.

3.2. Copper

Figures 3 and 4 display total and soluble copper concentration profiles, respectively. Total copper migration from the anodic zone is concluded since the copper concentration in partition 1 is significantly lower than, at least, two other partitions in each experiment. As with cobalt, partition 6 of experiment 4 has the highest total copper concentration amongst every partition in any experiment, reaching a 31.00% augmentation, which suggests that factor interaction is effective for this ion. In experiments 3 and 5, a higher concentration is found in partition 3, and the total copper concentration is not significantly different between these experiments in any partition. This suggests that there is no impact from the change of electric field or acid concentration at these levels. Moreover, when acid concentration is 1.0 mol L^{-1} , migration comes uniquely from partition 1, but when a higher solution is used, migration can pass through the cell, being the central zone for experiments 3 and 5 or partition 6 in experiment 4.

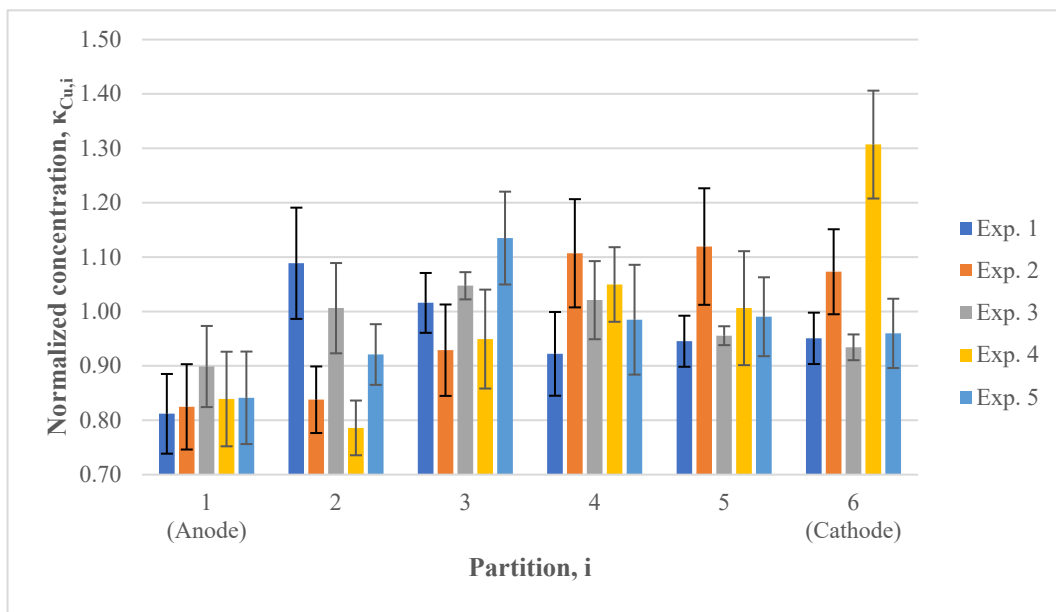


Figure 3. Total copper concentration.

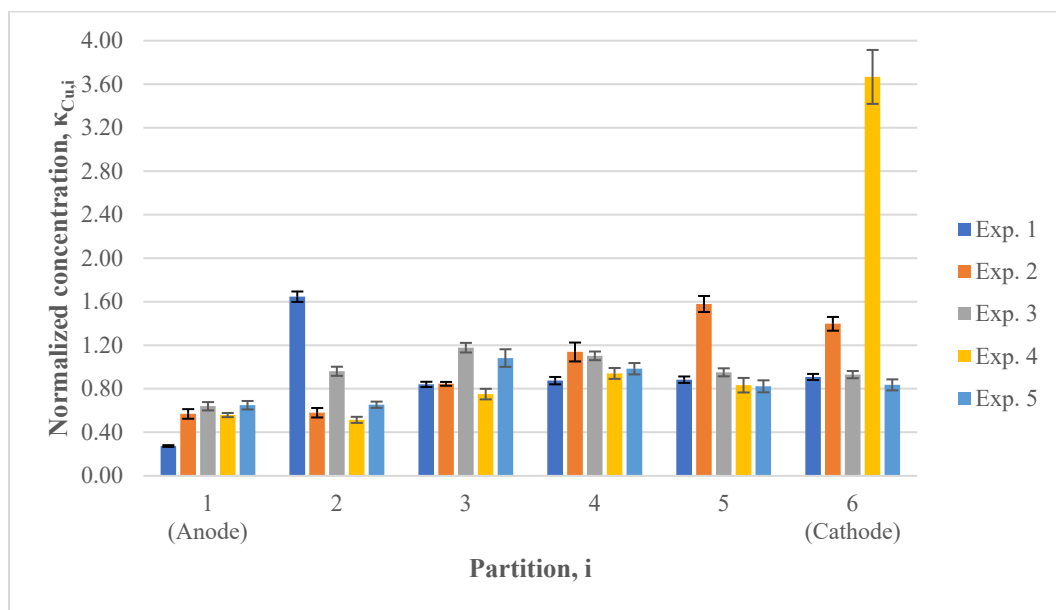


Figure 4. Soluble copper concentration.

Significant differences are proven throughout nearly the whole cell with regard to soluble copper, related to total copper profiles. Specifically, for partition 2 in experiment 1 and for partition 5 and 6 in experiment 2, soluble copper was 60% higher than initial concentrations, which suggests that, in the case of operating the EKR cell for more than seven days, copper migration to the cathodic zone could be significantly higher than observed here when the pretreatment solution was 1 mol L^{-1} . Nonetheless, in experiment 4, the weighted soluble copper proportion confidence interval throughout the cell was $32.95 \pm 4.03\%$, so copper solubilization is entirely evident in this case, since soluble copper is significantly higher than the initial concentration. This is supported by the understanding that IOCG ores present copper mainly as chalcopyrite, and for this mineralogical species, solubilization can happen when pH is between 2 and 4. There is an ORP higher than 0.3 V [36], which is the case, as was shown in a previous study [31] with the same ore and

operating conditions. The pH of experiments 2 and 4 was from 2.0 to 4.0 in almost the whole cell, which shows the highest total copper concentrations near the cathode.

3.3. Nickel

Figure 5 shows total nickel concentration profiles. In each experiment, the lowest concentration was found in partition 1 because all results in this partition, including their error bars, are below 1.0. A comparison between the partitions of an experiment shows that they presented lower confidence values than other partitions. In the experiments 2, 3, and 5, higher total nickel concentrations were found in half of the cell near the cathode, corresponding to partitions 4, 5, and 6. For experiment 4, nickel removal is observed in the anodic zone since partitions 1 and 2 have significantly lower nickel concentrations than at least three other partitions in the central and cathodic zones. That removed nickel migrated to partitions 4 through 6, the latter of which showed the highest concentration amongst any partition and experiment, reaching a 30.00% augmentation. This indicates that electromigration is significantly higher in these operation conditions than in others in this study. Furthermore, for this case, differences between experiments—excluding experiment 4—are very similar, with their bigger difference being the zone in the cell in which the highest concentrations were observed. This suggests that, with the aim of nickel removal, higher values of acid concentration and/or electric field or any other reagents could help nickel solubilization.

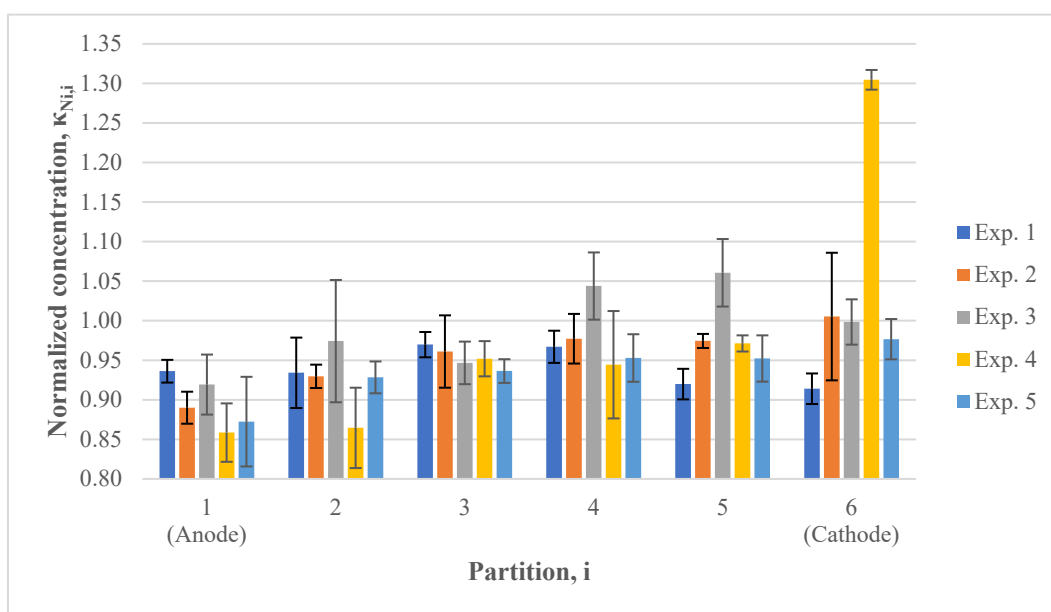


Figure 5. Total nickel concentration profiles.

With respect to soluble nickel, it was not possible to detect in most cases, including the original sample. Exceptions are partitions 2 and 3 in experiment 1, which had concentrations below 1.5 mg kg^{-1} , and in partition 6 from experiment 4, with $5.24 \pm 0.52 \text{ mg kg}^{-1}$. An explanation of this solubilization can be sustained by the work of Lewis [35], who established that nickel sulfides can be dissolved mildly when pH is below 4.0, that is, below 0.1 mg L^{-1} in solution. Thus, in the case of experiment 1, anodic nickel could partially dissolve and migrate to the central zone of the cell. In the case of experiment 4, when partition 1 had a pH value around 2.5—when solubilization can be in the order of 1.0 mg L^{-1} , according to Lewis—and partitions 2 through 5 had pH values below 4.0, nickel leaching was considerably higher, and nickel migration accumulated in the cathodic zone.

3.4. Metal Removal

Table 3 displays global removals for each metal in any experiment. For cobalt and nickel, a minimal removal could be obtained in experiments 1 and 5 in both cases. Furthermore, experiment 2 presents removal for nickel only, and experiment 3 shows a very minimal cobalt removal, as removal is significantly lower than in experiments 1 and 5, since in all those cases removal is higher than the confidence limit. If the experiments are compared, best cobalt removal can be achieved using 1.0 V cm^{-1} of electric field and 1.0 mol L^{-1} of acid solution, since experiment 1 shows significantly higher results than experiment 5. In the case of nickel, there is not a significant difference between the same experiments 1 and 5 since the confidence intervals share values; therefore, best results are achieved in the same conditions as cobalt.

Table 3. Global removal for each metal in every experiment.

	Experiments				
	1	2	3	4	5
Total removal _{Co}	7.19% ± 0.74%	0.15% ± 4.49%	2.38% ± 2.09%	−0.57% ± 3.53%	5.40% ± 0.74%
Total removal _{Cu}	4.05% ± 5.22%	1.82% ± 5.60%	2.27% ± 2.46%	−0.32% ± 6.80%	2.57% ± 0.74%
Total removal _{Ni}	5.95% ± 1.65%	4.07% ± 2.40%	0.84% ± 3.08%	0.39% ± 1.81%	6.33% ± 0.74%

Nonetheless, copper removal was not observed in any experiment. These results are coherent with a previous similar study [25], in which a relatively a fresh copper sulphide tailing was also treated, and global removal was not observed. In contrast to other studies in which copper was removed in EKR experiments [37,38], the principal difference in this study is the chemical compound in which copper is found, since copper used in those other experiments was a highly soluble one, such as CuSO_4 , which was added to the soil to form a synthetic sample. These findings, along with copper profiles, suggest solubilization can have a very important role in this kind of sample.

These indicators prove that, although experiment 4 shows better results in metal concentration, it is not the best combination to remove these metals from the cell. Even in the best conditions—experiment 1 for cobalt and nickel—nickel removal does not reach 2.0 mg kg^{-1} recovery, and cobalt obtains around 6.4 mg kg^{-1} . Nonetheless, these experimental runs were made for seven days. Thus, a potentially important removal could have been made if the experiment had been extended for more time, especially when each species was concentrated over 10% in the cathodic zone.

3.5. Interaction Proof

ANOVA *p*-value results for each metal are shown in Table 4. For cobalt, the effect of the electric field, pretreatment solution concentration, and their interaction is proven in partition 6. In partition 3, initial acidity has a relevant effect, while interaction between factors is proven in partitions 4 through 6. Nonetheless, factor effects in partitions 1 and 2 are not apparent.

For total copper, the electric field had a validated effect in partition 2, and sulfuric acid concentration had an incidence in each partition except partition 1. As with cobalt, factor interaction is proven in the same half-cell, and all factors and interactions are proven in partition 6. Furthermore, partition 1 shows no evidence of any factor influence. Regarding soluble copper, every factor and interaction influenced it throughout the entire cell, with the exception being partition 4, the factor interaction of which had an incidence in soluble copper concentration.

In the case of nickel, the initial acidity effect was shown throughout the cell, except in partition 3. Electric field incidence was proven in partitions 1, 5, and 6, and factor interaction was noted in partitions 2, 4, 5, and 6. As with every other species, each factor and its interaction incidences were shown in partition 6.

Table 4. Calculated *p*-values of each factor and their interaction for each partition.

Metal	Variability Source	Partition					
		1	2	3	4	5	6
Cobalt	Electric Field	60.70%	31.95%	71.70%	66.52%	13.35%	0.03%
	Initial Acidity	13.13%	10.09%	0.74%	16.93%	16.77%	0.02%
	Interaction	45.10%	14.54%	30.79%	3.09%	5.48%	4.80%
Total Copper	Electric Field	15.51%	6.95%	30.05%	48.71%	12.38%	0.33%
	Initial Acidity	46.24%	0.10%	1.33%	1.66%	1.33%	0.01%
	Interaction	27.77%	60.64%	81.29%	4.42%	8.02%	0.20%
Soluble Copper	Electric Field	0.02%	0.00%	0.52%	78.25%	0.01%	0.00%
	Initial Acidity	0.41%	0.00%	0.05%	15.86%	0.02%	0.00%
	Interaction	0.03%	0.00%	0.03%	0.09%	0.00%	0.00%
Nickel	Electric Field	8.37%	58.22%	20.50%	27.25%	0.08%	0.35%
	Initial Acidity	0.71%	5.27%	87.38%	6.20%	7.87%	0.03%
	Interaction	52.58%	6.60%	54.89%	3.40%	0.06%	0.04%

These results indicate that no matter which operating conditions are used, cobalt and copper are affected indifferently in the partition nearest to the anode, which suggests that proton formation in the anode and migration should be more effective in their solubilization and migration but in two opposite directions, such that copper solubilization is important, and cobalt has almost null solubilization. For nickel, the effect of acid could be explained by considerably higher solubilization with a lower pH in the conditions of these experiments.

Additionally, as in partition 6, every effect and interaction was proven; the inference is that, as metal migration goes directly to the cathode, every metal liberation and/or migration process, as mild as it could be, accumulates its effect in the partition near the cathode, even more so when metal removal was almost nonexistent in the experiments. Thus, if the operation aims to accumulate the species in a narrower section, each factor has a significant effect and its interaction as a declared enhancement.

According to ANOVA tests, factor interaction was proven by obtaining *p*-values below 10% in three partitions for each metal, being the closest to the cathode (partitions 4, 5, and 6). In partition 6 specifically, both main factors affected metal concentrations. In the case of cobalt and copper, in partition 1, neither the factor nor their interaction affected their total concentrations, which suggested that electrolysis in the anode is more determinant than the solubilization and/or migration of these metals in this zone. Regarding nickel, pretreatment solution concentration has proven effective in this partition since solubilization is considerably higher at the lower pH values of this experiment.

4. Conclusions

Although copper removal was not observed in any experiment, approximately 7.19% of cobalt and 5.95% of nickel were removed using 1.0 V cm^{-1} of electric field and 1.0 mol L^{-1} of pretreatment solution. Nonetheless, for each species, a concentration augmentation was achieved in partition 6, reaching 11.00% for cobalt, 31.00% for copper, and 30.00% for nickel, all of which were observed when the electric field was at 2.0 V cm^{-1} and the pretreatment solution was at 2.0 mol L^{-1} . It is highly recommended to repeat the experiments for, at least, twice the time used in this study since there is evidence of high metal concentration in the cathodic zone, which may be removed from the cell in that amount of time. Additionally, solubilization has a very important role in this kind of samples, and it is highly recommended to assess it separately from migration phenomena.

Regarding the ANOVA tests, interaction between the factors was proven in half of the cell near the cathode by having *p*-values below 10% in those partitions. Moreover, every factor and interaction for all species was observed in partition 6. Regarding nickel, pretreatment concentration reduces its concentration almost throughout the EKR cell. With regard to electric field, its incidence was proven in fewer partitions than initial acidity.

Therefore, a migration enhancement was obtained when electric field was at 2.0 V cm^{-1} and pretreatment solution was at 2.0 mol L^{-1} , with the aim of collecting more of each species near the cathode. A replication of the experiments with a longer operation time is strongly suggested to observe a better removal rate.

Author Contributions: Conceptualization, R.O.-S. and H.H.; methodology, C.G.; software, R.O.-S.; validation, A.A., H.H. and L.O.; formal analysis, R.O.-S.; investigation, D.L.; resources, A.L.; data curation, P.L.; writing—original draft preparation, R.O.-S. and M.L.; writing—review and editing, D.L. and M.L.; visualization, C.G.; supervision, H.H.; project administration, H.H.; funding acquisition, A.A. All authors have read and agreed to the published version of the manuscript.

Funding: This research received no external funding.

Institutional Review Board Statement: Not applicable.

Informed Consent Statement: Not applicable.

Data Availability Statement: Not applicable.

Conflicts of Interest: The authors declare no conflict of interest.

References

1. Lacasa, E.; Cotillas, S.; Saez, C.; Lobato, J.; Canizares, P.; Rodrigo, M.A. Environmental applications of electrochemical technology. What is needed to enable full-scale applications? *Curr. Opin. Electrochem.* **2019**, *16*, 149–156. [[CrossRef](#)]
2. Kelm, U.; Helle, S.; Matthies, R.; Morales, A. Distribution of trace elements in soils surrounding the El Teniente porphyry copper deposit, Chile: The influence of smelter emissions and a tailings deposit. *Environ. Geol.* **2009**, *57*, 365–376. [[CrossRef](#)]
3. Ramirez, M.; Massolo, S.; Frache, R.; Correa, J.A. Metal speciation and environmental impact in Sandy beaches due to El Salvador copper mine, Chile. *Mar. Pollut. Bull.* **2005**, *50*, 62–72. [[CrossRef](#)]
4. Fernández-Marchante, C.M.; Souza, F.L.; Millán, M.; Lobato, J.; Rodrigo, M.A. Can the green energies improve the sustainability of electrochemically-assisted soil remediation processes? *Sci. Total Environ.* **2022**, *803*, 149991–149999. [[CrossRef](#)] [[PubMed](#)]
5. Figueroa, A.; Cameselle, C.; Gouveia, S.; Hansen, H.K. Electrokinetic treatment of an agricultural soil contaminated with heavy metals. *J. Environ. Sci. Health A Tox. Hazard. Subst. Environ. Eng.* **2016**, *51*, 691–700. [[CrossRef](#)] [[PubMed](#)]
6. Correa, J.A.; Castilla, J.C.; Ramirez, M.; Varas, M.; Lagos, N.; Vergara, S.; Moenne, A.; Roman, D.; Brown, M.T. Copper, copper mine tailings and their effect on marine algae in northern Chile. *J. Appl. Physiol.* **1999**, *11*, 57–67. [[CrossRef](#)]
7. Leysens, L.; Vinck, B.; Van Der Straeten, C.; Wuyts, F.; Maes, L. Cobalt toxicity in humans—A review of the potential sources and systemic health effects. *Toxicology* **2017**, *387*, 43–56. [[CrossRef](#)] [[PubMed](#)]
8. Schaumlöffel, D. Nickel species: Analysis and toxic effects. *J. Trace Elem. Med. Biol.* **2012**, *26*, 1–6. [[CrossRef](#)]
9. Vardhan, K.H.; Kumar, P.S.; Panda, R.C. A review on heavy metal pollution, toxicity and remedial measures: Current trends and future perspectives. *J. Mol. Liq.* **2019**, *290*, 111197–111218. [[CrossRef](#)]
10. Araya, N.; Mamani Quiñonez, O.; Cisternas, L.A.; Kraslawski, A. Sustainable Development Goals in Mine Tailings Management: Targets and Indicators. *Mater. Proc.* **2021**, *5*, 82. [[CrossRef](#)]
11. Aznar-Sánchez, J.A.; García-Gómez, J.J.; Velasco-Muñoz, J.F.; Carretero-Gómez, A. Mining Waste and Its Sustainable Management: Advances in Worldwide Research. *Minerals* **2018**, *8*, 284. [[CrossRef](#)]
12. Qin, J.; Zhao, H.; Dai, M.; Zhao, P.; Chen, X.; Liu, H.; Lu, B. Speciation Distribution and Influencing Factors of Heavy Metals in Rhizosphere Soil of Miscanthus Floridulus in the Tailing Reservoir Area of Dabaoshan Iron Polymetallic Mine in Northern Guangdong. *Processes* **2022**, *10*, 1217. [[CrossRef](#)]
13. Tarfeen, N.; Nisa, K.U.; Hamid, B.; Bashir, Z.; Yattoo, A.M.; Dar, M.A.; Mohiddin, F.A.; Amin, Z.; Ahmad, R.A.; Sayyed, R.Z. Microbial Remediation: A Promising Tool for Reclamation of Contaminated Sites with Special Emphasis on Heavy Metal and Pesticide Pollution: A Review. *Processes* **2022**, *10*, 1358. [[CrossRef](#)]
14. Liu, L.; Li, W.; Song, W.; Guo, M. Remediation techniques for heavy metal-contaminated soils: Principles and applicability. *Sci. Total Environ.* **2018**, *633*, 206–219. [[CrossRef](#)]
15. Acar, Y.B.; Gale, R.J.; Alshawabkeh, A.N.; Marks, R.E.; Puppala, S.; Bricka, M.; Parker, R. Electrokinetic remediation: Basics and technology status. *J. Hazard. Mater.* **1995**, *40*, 117–137. [[CrossRef](#)]
16. Alshawabkeh, A.N. Electrokinetic soil remediation: Challenges and oportunitites. *Sep. Sci. Technol.* **2009**, *44*, 2171–2187. [[CrossRef](#)]
17. Singh, A.; Kuhad, R.C.; Ward, O.P. Biological Remediation of Soil: An Overview of Global Market and Available Technologies. In *Advances in Applied Bioremediation; Soil Biology*; Singh, A., Kuhad, R., Ward, O., Eds.; Springer: Berlin/Heidelberg, Germany, 2009; Volume 17, ISBN 978-3-540-89621-0.
18. Boonmeerati, U.; Sampanpanish, P. Enhancing Arsenic Phytoextraction of Dwarf Napier Grass (*Pennisetum purpureum* cv. Mott) from Gold Mine Tailings by Electrokinetics Remediation with Phosphate and EDTA. *J. Hazard. Toxic Radioact. Waste* **2021**, *25*, 04021027. [[CrossRef](#)]

19. Torabi, M.S.; Asadollahfardi, G.; Rezaee, M.; Panah, N.B. Electrokinetic Removal of Cd and Cu from Mine Tailing: EDTA Enhancement and Voltage Intensity Effects. *J. Hazard. Toxic Radioact. Waste* **2021**, *25*, 05020007. [[CrossRef](#)]
20. Asadollahfardi, G.; Sarmadi, M.S.; Rezaee, M.; Khodadadi-Darban, A.; Yazdani, M.; Paz-Garcia, J.M. Comparison of different extracting agents for the recovery of Pb and Zn through electrokinetic remediation of mine tailings. *J. Environ. Manag.* **2021**, *279*, 111728–111739. [[CrossRef](#)]
21. Boonmeerati, U.; Sampanpanish, P. Application of Phosphate and EDTA on As(V) Removal in Gold Mine Tailings by Electrokinetic Remediation. *EnvironmentAsia* **2020**, *13*, 1–12. [[CrossRef](#)]
22. Kirkelund, G.M.; Jensen, P.E.; Ottosen, L.M.; Pedersen, K.B. Comparison of two- and three-compartment cells for electro-dialytic of heavy metals from contaminated material suspensions. *J. Hazard. Mater.* **2019**, *367*, 68–76. [[CrossRef](#)] [[PubMed](#)]
23. Rosa, M.A.; Egido, J.A.; Márquez, M.C. Enhanced electrochemical removal of arsenic and heavy metals from mine tailings. *J. Taiwan. Inst. Chem. E.* **2017**, *78*, 409–415. [[CrossRef](#)]
24. Demir, A.; Pamukcu, S.; Shrestha, R.A. Simultaneous Removal of Pb, Cd, and Zn from Heavily Contaminated Mine Tailing Soil Using Enhanced Electrochemical Process. *Environ. Eng. Sci.* **2015**, *32*, 416–424. [[CrossRef](#)]
25. Hansen, H.K.; Lamas, V.; Gutiérrez, C.; Nuñez, P.; Rojo, A.; Cameselle, C.; Ottosen, L.M. Electro-remediation of copper mine tailings. Comparing copper removal efficiencies for two tailings of different age. *Miner. Eng.* **2013**, *41*, 1–8. [[CrossRef](#)]
26. Hansen, H.K.; Rojo, A.; Ottosen, L.M. Electrokinetic remediation of copper mine tailings—Implementing bipolar electrodes. *Electrochim. Acta* **2007**, *52*, 3355–3359. [[CrossRef](#)]
27. Hansen, H.K.; Rojo, A. Testing pulsed electric fields in electroremediation of copper mine tailings. *Electrochim. Acta* **2007**, *52*, 3399–3405. [[CrossRef](#)]
28. Jensen, P.E.; Ottosen, L.M.; Hansen, H.K.; Bollwerk, S.; Belmonte, L.J.; Kirkelund, G.M. Suspended electro-dialytic extraction of toxic elements for detoxification of three different mine tailings. *Int. J. Sustain. Dev. Plan.* **2016**, *11*, 119–127. [[CrossRef](#)]
29. Hansen, H.K.; Rojo, A.; Ottosen, L.M. Electro-dialytic remediation of copper mine tailings. *J. Hazard. Mater.* **2005**, *117*, 179–183. [[CrossRef](#)]
30. Rojo, A.; Hansen, H.K.; Ottosen, L.M. Electro-dialytic remediation of copper mine tailings: Comparing different operational conditions. *Miner. Eng.* **2006**, *19*, 500–504. [[CrossRef](#)]
31. Ortiz-Soto, R.; Leal, D.; Gutierrez, C.; Aracena, A.; Rojo, A.; Hansen, H.K. Electrokinetic remediation of manganese and zinc in copper mine tailings. *J. Hazard. Mater.* **2019**, *365*, 905–911. [[CrossRef](#)]
32. Del Real, I.; Thompson, J.F.H.; Simon, A.C.; Reich, M. Geochemical and Isotopic Signature of Pyrite as a Proxy for Fluid Source and Evolution in the Candelaria-Punta del Cobre Iron Oxide Copper-Gold District, Chile. *Econ. Geol.* **2020**, *115*, 1493–1518. [[CrossRef](#)]
33. Montgomery, D.C.; Runger, G.C. *Applied Statistics and Probability for Engineers*, 7th ed.; Wiley: Hoboken, NJ, USA, 2018; ISBN 978-1-119-40036-3.
34. Papadopoulos, C.E.; Yeung, H. Uncertainty estimation and Monte Carlo method. *Flow Meas. Instrum.* **2001**, *12*, 291–298. [[CrossRef](#)]
35. Lewis, A.E. Review of metal sulphide precipitation. *Hydrometallurgy* **2010**, *104*, 222–234. [[CrossRef](#)]
36. Córdoba, E.M.; Muñoz, J.A.; Blázquez, M.L.; González, F.; Ballester, A. Leaching of chalcopyrite with ferric ion. Part I: General aspects. *Hydrometallurgy* **2008**, *93*, 81–87. [[CrossRef](#)]
37. Chen, R.; Zhou, L.; Wang, W.; Cui, D.; Hao, D.; Guo, J. Enhanced Electrokinetic Remediation of Copper-Contaminated Soil by Combining Steel Slag and a Permeable Reactive Barrier. *Appl. Sci.* **2022**, *12*, 7981. [[CrossRef](#)]
38. Ge, X.; Xie, J.; Song, X.; Cao, X.; Wang, Y.; Xu, Z. Electrokinetic Remediation of Cadmium (Cd), Copper (Cu) and Nickel (Ni) Co-contaminated soil with Oxalic Acid, Acetic Acid or Citric Acid as a Catholyte. *Int. J. Electrochem. Sci.* **2022**, *17*, 220444. [[CrossRef](#)]

Disclaimer/Publisher’s Note: The statements, opinions and data contained in all publications are solely those of the individual author(s) and contributor(s) and not of MDPI and/or the editor(s). MDPI and/or the editor(s) disclaim responsibility for any injury to people or property resulting from any ideas, methods, instructions or products referred to in the content.